SECOND EUROPEAN CONFERENCE ON EARTHQUAKE ENGINEERING
AND SEISMOLOGY, ISTANBUL AUG. 25-29, 2014

THE ROLE OF SUPPLEMENTAL DAMPING IN LIMITING FORCES AND DISPLACEMENTS IN A ROCKING STRUCTURE

Sinan ACIKGOZ[1], Andrew ARGYLE[2] and Matthew DEJONG[3]

The effectiveness of rocking mechanisms fundamentally relies on the ability of rocking action to limit the inertial forces on the superstructure. Previous experimental and analytical studies have drawn attention to significant drift demands and large lateral accelerations that might arise during rocking action. In many rocking structures, dampers are used at the rocking interface. The aim of this paper is to investigate the effect of such dampers on the displacement and force demands. The Christchurch Rocking Chimney is considered as a case study, and is modeled using a large deformation analytical model that is herein extended to incorporate the effect of dampers. Simulation results indicate that the dampers have a negligible effect for small and moderate ground motions, while they effectively limit rocking rotation for larger ground motions. Finally, a parametric study that investigates both the damper characteristics and the superstructures stiffness provides more general insight regarding the seismic response of flexible rocking structures with supplemental damping.

INTRODUCTION

There is an increasing demand in the field of earthquake engineering to design structures that are not only safe, but that also limit and locate damage during an earthquake to avoid post-earthquake demolition. Various new systems are being proposed with this aim, including extensive research on the use of rocking (or stepping) to isolate the structure from the ground motion (see Hajjar et al. 2013 for a review of related experimental investigations).

The dynamics of rocking structures have been investigated in some detail, and the beneficial effects of rocking isolation have been demonstrated both experimentally and analytically (e.g. Yim and Chopra, 1985). However, experimental studies have identified the potential for significant higher mode vibrations to be directly excited by the ground motion itself (e.g. Wiebe et al. 2013), or for impacts during rocking to illicit a large vibration response (e.g. Toranzo-Dianderas 2002). Recent experimental and analytical studies by the authors (Acikgoz et al. 2014, Acikgoz and DeJong 2014) have investigated superstructure vibrations of freely rocking structures, and characterized the vibrations during rocking motion.

In practice, many proposed systems that employ rocking use energy dissipaters at the location of uplift. An example of such a structure is the Christchurch Chimney in Fig. 1. The chimney was designed to rock at the interface between the superstructure and the foundation, where metallic plates were installed to provide hysteretic damping during rocking. During rocking, the assumed critical axis of rotation lies through the end of two of the four 'legs' of the structure (axis A-A, Fig. 1).

The objective of this paper is to investigate the response of the Christchurch Chimney to earthquake ground motion, and to investigate the effects of the hysteretic dampers on the rocking response. The analytical model employed is first presented, followed by the characteristics of the chimney, the damper, and the dynamics of the entire system. The model is then used to evaluate the rocking response of the chimney to various earthquake records. Finally, the model is used to more

[1] PhD candidate, University of Cambridge, Cambridge, msa44@cam.ac.uk
[2] MEng candidate, University of Cambridge, Cambridge, aa633@cam.ac.uk
[3] Lecturer, University of Cambridge, Cambridge, mjd97@cam.ac.uk

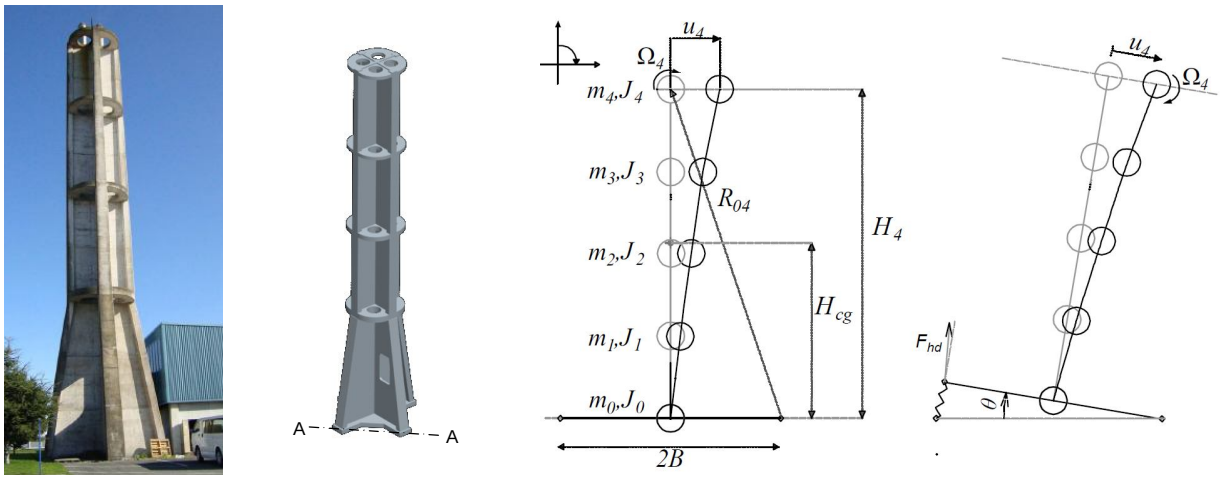

Figure 1. Photo of the Christchurch chimney (after Sharpe and Grinlinton, 2013), ProEngineer model of the chimney indicating rocking axis A-A, and the MDOF analytical model for the full contact and rocking phases of motion

generally investigate the effects of the characteristics of the hysteretic dampers and the superstructure on the seismic response, in order to inform future design of similar systems.

ANALYTICAL MODEL

The non-smooth analytical model utilized in this study is illustrated in Fig. 1 (right) for both the full contact and rocking phases. It is a modified from an earlier model which describes the large rocking response of a generic multi degree of freedom (MDOF) structure on rigid ground (Acikgoz and DeJong, 2014). For modeling the chimney, hysteretic dampers were added at the structure-foundation interface and the equations of motion governing the response are discussed in this section.

The analytical model is comprised of 5 nodes where masses are lumped. The top node, identified as node 4, has a height of H_4 and a mass of m_4 (Fig. 1), while the bottom node, identified as node 0, is located at the foundation beam, $H_0 = 0$, with mass m_0. Rotational masses (denoted by J_j in Fig. 1) are assumed zero. All masses are allowed to displace horizontally and rotate (illustrated by u_4 and Ω_4 for node 4 in Fig. 1), except for the foundation beam. The nodes are connected by inextensible Euler beam elements. These elements implicitly consider the effects of rotational end stiffness, in the form of condensed stiffness and mass matrices (Acikgoz and DeJong, 2014). The modulus of elasticity of concrete (E) and the uncracked sectional moment of inertia (I) of the composite section is utilized in formulating the input parameters for these beams (Table 1). Then, by using Rayleigh damping, characterized by 3.5% damping ratio for the first two modes, the damping matrix for the full contact phase is constructed.

Similar to the chimney, where rocking is expected to occur about contact areas concentrated on edge lead pads, pivot axes about which rocking could occur were defined in the model. The current pivot axis about which rotation occurs is denoted by subscript p and the impending pivot axis is described by subscript p'. These pivot axes are parallel and are a distance of $2B$ apart, and both lie at a distance of R_{04} from the inertial position of node 4. The structure is assumed to maintain contact with one of the pivot axes during the entire rocking motion. Therefore, a vector of relative elastic displacements for nodes 1-4, denoted by $\underline{u}$, and a rocking angle parameter θ suffice to describe the motion. Uplift and the subsequent rocking motion are restrained by the presence of a non-degrading hysteretic metallic damper (Tyler, 1978), which was modeled using a Bouc-Wen hysteresis model (Wen, 1976).

Throughout this paper differentiation of Lagrangian coordinates with respect to time is denoted by dots over the variables. Equations are typically expressed in implicit form with matrix notation

where matrices are denoted in brackets and vectors are underlined. Using these notations, the small elastic displacement response of the structure in full contact phase is described by the well-known equations below:

$$[M]\left(\underline{\ddot{u}} + \underline{1}\ddot{u}_g\right) + [C]\underline{\dot{u}} + [K]\underline{u} = 0 \tag{1}$$

where 4×4 mass, damping and stiffness matrices for nodes 1-4 are denoted respectively by $[M]$, $[C]$ and $[K]$, $\ddot{u}_g$ describes the ground accelerations, and $\underline{1}$ is a 4×1 vector of ones. When the overturning moment about the impending pivot axis p' exceeds the restraining moment about the same corner, uplift may occur. It is additionally required that the angular momentum about the impending pivot axis (denoted by $L_{p'}^{fc}$) should be in the direction of rocking motion. These conditions are expressed as follows:

$$\mp\underline{H}^T[M]\left(\underline{\ddot{u}} + \underline{1}\ddot{u}_g\right) > \underline{1}^T[M]\left(B\underline{1} \mp \underline{u}\right)g + m_0 gB \pm F_{hd}(2B) \tag{2}$$

$$\pm L_{p'}^{fc} = \pm\underline{H}^T[M]\underline{\dot{u}} > 0 \tag{3}$$

where g is the gravitational acceleration and the vector $\underline{H}$ contains the heights of the nodes. The force exerted on the edge of the rigid foundation beam by the active hysteretic damper is denoted by F_{hd} in Eq. 2. During full contact (no rocking), an active hysteretic damper refers to the damper which exerts a moment about the impending pivot axis p'. Note that the lower sign denotes rocking about left pivot axis and the upper sign denotes rocking about the right pivot axis (see for example, Fig. 1). A similar notation is used throughout this paper.

When the uplift conditions in Eqs. 2 and 3 are satisfied, a rocking phase commences. The initial conditions of the rocking phase are identical to the final conditions of the full contact phase. Three sets of differential equations describe the dynamic equilibrium during rocking: (i) Dynamic force equilibrium in the direction of $\underline{u}$ for each node, (ii) dynamic moment equilibrium about the system pivot axis and (iii) hysteretic behavior of the damper. The first set of equations is given by:

$$[M]\underline{\ddot{u}} + [M]\underline{1}\ddot{u}_g\cos\theta + [M]\underline{H}\ddot{\theta} + [M](\pm B\underline{1} - \underline{u})\dot{\theta}^2 + [C]\underline{\dot{u}} + [K]\underline{u} + [M]\underline{1}g\sin\theta = 0 \tag{4}$$

The second differential equation is given as:

$$\begin{aligned}&\left(J_p + \underline{u}^T[M]\underline{u} \mp 2B\,\underline{1}^T[M]\underline{u}\right)\ddot{\theta} + \underline{H}^T[M]\underline{\ddot{u}} \mp 2\dot{u}^T[M](B\,\underline{1} \mp \underline{u})\dot{\theta}\\ &+F_{hd}(2B\cos(\theta/2)) + \ddot{u}_g\left(\underline{H}^T[M]\underline{1}\cos\theta \pm \underline{1}^T[M]\left(B\,\underline{1} \mp \underline{u}\right)\sin\theta \pm m_0 B\sin\theta\right)\\ &+g\left(-\underline{H}^T[M]\,\underline{1}\sin\theta \pm \underline{1}^T[M]\left(B\,\underline{1} \mp \underline{u}\right)\cos\theta \pm m_0 B\cos\theta\right) = 0\end{aligned} \tag{5}$$

where $J_p = m_0B^2 + \underline{R_0}^T[M]\underline{R_0}$ is the mass moment of inertia of the structure at rest position about the pivot axis. The force exerted on the uplifted edge of the rigid foundation beam by the hysteretic damper is denoted by F_{hd}, and is the only damper that is active during a rocking cycle. Force might have been stored in the damper located near the pivot axis during a previous rocking cycle, but the effects of this force on rocking motion are only observed when this damper is activated at the initiation of a new rocking cycle. During a rocking cycle, the force exerted by the active damper F_{hd} is given by:

$$F_{hd} = k_{hd}\varepsilon_{hd}\left(4B\sin\frac{\theta}{2}\right) + k_{hd}(1-\varepsilon_{hd})\left(4B\sin\frac{\theta_y}{2}\right)z \tag{6}$$

where k_{hd} is the pre-yield stiffness of the damper, ε_{hd} is the ratio of the post-yield to pre-yield stiffness, θ_y is the rocking angle at which the hysteretic dampers yield, and z is the hysteretic parameter which is recorded separately for both dampers. For the active damper, z is determined by the following differential equation:

$$\left(4B\sin\frac{\theta_y}{2}\right)\dot{z}+\alpha\left|2B\dot{\theta}\cos\left(\frac{\theta}{2}\right)\right|z|z|^{n-1}+\beta\left(2B\dot{\theta}\cos\left(\frac{\theta}{2}\right)\right)|z|^{n}-2B\dot{\theta}\cos\left(\frac{\theta}{2}\right) \tag{7}$$

Eqs. 4-7 describe the smooth equations of motion that govern a rocking phase. These equations are terminated when $\theta=0$ and the structure impacts the ground. The duration of this impact is assumed to be much smaller than the vibration frequencies of the structure. Therefore, the rocking velocities, which are assumed to be uncoupled from elastic displacements during impact, may be decreased or completely dissipated. Conversely, in the absence of external forcing, elastic displacements and velocities are assumed to remain constant during impact. As the chimney model rests on soft lead pads, a more accurate model would require the evaluation of the coupling of impact forces and elastic motion. Generally, this coupling would lead to a reduction of elastic displacement demand on the system. Therefore, the 'classical impact' approach adopted in this paper may lead to a conservative estimate of the vibrations that arise due to impact (for a more detailed investigation, refer to Acikgoz and DeJong, 2014).

Two conditions are used to determine the phase of motion following impact. Similar to Eq. 3, the first condition evaluates the angular momentum about the impending pivot axis, $L^r_{p'}$. The second condition sets a minimum rocking velocity to proceed to the next phase in order to prevent numerical instability. The two conditions are:

$$\begin{aligned}&\mp L^r_{p'}\geq 0\\&\mp\dot{\theta}^{-}>0.0015\end{aligned} \tag{8}$$

where the superscripts $^-$ and $^+$ denote the pre- and post-impact parameters. There are two possible outcomes. If the conditions presented in Eq. 8 are not satisfied, then a full contact phase is assumed to begin. During this non-smooth transition, the vertical momentum is completely dissipated, while the horizontal momentum at each node is assumed to be conserved. Therefore the post-impact parameters are given as $\dot{\theta}^{+}=0$, $\underline{\dot{u}}^{+}=\underline{\dot{u}}^{-}+\underline{H}\dot{\theta}^{-}$. If the conditions in Eq. 8 are satisfied, then a new rocking phase is initiated about the impending pivot axis. The post-impact parameters are then given as $\dot{\theta}^{+}=r\dot{\theta}^{-}$, $\underline{\dot{u}}^{+}=\underline{\dot{u}}^{-}$ where r is a coefficient of restitution. In this case, the post-impact value of z^{+} assumes the final value recorded during the previous rocking cycle about the same pivot axis.

Assuming that the impact forces are concentrated at the impending pivot axis, angular momentum about this corner may be conserved during impact. Using this principle, a conservative approximation of r may be made to estimate the coefficient of restitution:

$$r=\frac{\dot{\theta}^{+}}{\dot{\theta}^{-}}=\frac{L^r_{p'}}{L^r_{p}}=\frac{\left(J_p-2(\underline{1}^T[M]\underline{1}+m_0)B^2+\underline{u}^T[M]\underline{u}\right)\dot{\theta}+\underline{H}^T[M]\underline{\dot{u}}}{\left(J_p\mp 2B(\underline{1}^T[M]\underline{u})+\underline{u}^T[M]\underline{u}\right)\dot{\theta}+\underline{H}^T[M]\underline{\dot{u}}} \tag{9}$$

When the elastic displacements are assumed small, $\underline{u}\approx\underline{0}$, Eq. 9 becomes:

$$r\approx\frac{\left(J_p-2(\underline{1}^T[M]\underline{1}+m_0)B^2\right)}{J_p} \tag{10}$$

Eq. 9 provides an estimate of the coefficient of restitution factors, using the displaced state of the structure at the moment of impact. As the elastic displacements are typically small, r may be estimated using the geometrical characteristics of the structure shown in Eq. 10. This equation shows the important nature of geometric characteristics in determining the energy loss during an impact.

In this paper, Eq. 1 was used to simulate the full contact phase and Eqs. 4-7 were used to simulate the rocking phases of motion. Eqs. 4-7 demonstrate significant mass and stiffness coupling as well as geometric nonlinearity due to rocking. These equations were numerically solved in MATLAB using implicit ODE solvers (Shampine et al., 2003). The phase transition conditions in Eqs. 2-3 and 9-10 are evaluated using the event recognition capability of these solvers. To complement these numerical simulations it is useful to linearize the governing equations of motion (see Acikgoz and DeJong 2013 for details of the linearization for a similar system). These linearized equations are not presented here for brevity, but are utilized in the following section to provide a clearer understanding of the dynamic characteristics of the system.

In the following sections, the displacement and force demands on the structure are presented for different earthquake records. In order to effectively evaluate the response, non-dimensional displacement and force demand terms were defined. The two displacement demand terms considered, the total top node displacement and the elastic top node displacement, were normalized by H_4, the top node height. These are given by:

$$\delta_t = \left(\pm B(1-\cos\theta) + u_4\cos\theta + H_4\sin\theta\right)/H_4 = \delta_4/H_4 \tag{11}$$

$$\delta_e = \left(u_4\cos\theta\right)/H_4 \tag{12}$$

Meanwhile, the overturning moments and shear forces were normalized by reference values, defined as the base shear V_{ref} and overturning moment M_{ref} at the critical displacement which would cause a first-mode dominated structure to uplift when $F_{hd} = 0$ (Acikgoz and DeJong, 2012). Thus, these normalized parameters essentially illuminate the portion of the response after rocking is initiated.

MODEL PARAMETERS

The input parameters required for the analytical modelling are defined in Table 1. The majority of the chimney parameters were either extracted from the ProEngineer model shown in Fig. 1 (middle), which was created from original construction drawings, or were calculated by hand directly from the geometry. Note that an average sectional moment of inertia was assumed for the bottom tapered portion of the chimney, and the value of the concrete Young's Modulus was also assumed as typical.

The characteristics of the hysteric dampers were never measured directly, so no data was available to directly define the necessary related input parameters. However, Fig. 2 (top left) depicts a tapered metallic damper that was tested cyclically (Fig. 2, top right), and is similar in geometry to the damper installed in the chimney (Fig. 2, bottom). The Bouc-Wen model described above was first fit to best match the cyclic experimental results (Fig. 2, top right). Then, to approximate the parameters needed for the chimney dampers, it was assumed that the values of ε_{hd}, α, β and C from the fitting results would be good estimates, while k_{hd} and d_{y0} were directly calculated from the specific geometry of the chimney dampers.

The linearized equations of motion mentioned in the previous section were first used to evaluate the dynamic characteristics of the chimney, before considering the response to earthquake motion. Fig. 3 presents the numerical results of an eigenvalue analysis using the linearized equations. For each mode, both the mode shapes and frequencies of the fixed base structure and the rocking structure are compared. For mode one, the fixed base frequency is 2.18 Hz, while the vibration frequency during rocking is 6.22 Hz. Additionally, the vibration mode during rocking induces a rotation of the base. These effects have recently been observed experimentally and indicate a significant change in vibration characteristics during rocking (Acikgoz et al. 2014). For higher modes, the difference of

Table 1. Model input parameters

Part	Parameter	Value	Definition
Chimney	B (m)	3.3	Half-distance between pivot axes
	$\underline{H}$ (m)	[10.4; 17.95; 25.5; 33.05]	Heights of nodes
	$\underline{M}$ (t)	[78.6; 60.8; 53.8; 31.0]	Masses at nodes corresponding to $\underline{H}$ vector
	m_0 (t)	62.4	Mass at zero height
	$\underline{I}$ (m^4)	[9.84; 4.03; 3.45; 3.01]	Sectional second moment of area between each node
	J_p (kg-m^2)	10^8	Total mass moment of inertia about rocking pivot
	H_{cg} (m)	15.0	Height of the centre of gravity
	α_{cg} (rad)	0.216	Slenderness angle of the centre of gravity
	r (-)	0.94	Coefficient of restitution estimate (see Eq.10)
	E (Gpa)	20	Assumed Young's modulus of concrete
Hysteretic Damper	k_{hd} (kN/m)	10^7	Initial damper stiffness
	ε_{hd} (-)	0.06	Ratio of post-yield to pre-yield damper stiffness
	d_{y0} (mm)	3.74	Approximate damper displacement at initial yielding
	d_y (mm)	18.7	Damper displacement at full yielding
	C (-)	5	Ratio of full yielding to initial yielding displacement
	θ_y (rad)	2.8 x 10^{-3}	Rotation of chimney base at full yielding
	α (-)	1.0	Bouc-Wen model parameter
	β (-)	0	Bouc-Wen model parameter
	n (-)	1	Bouc-Wen model parameter

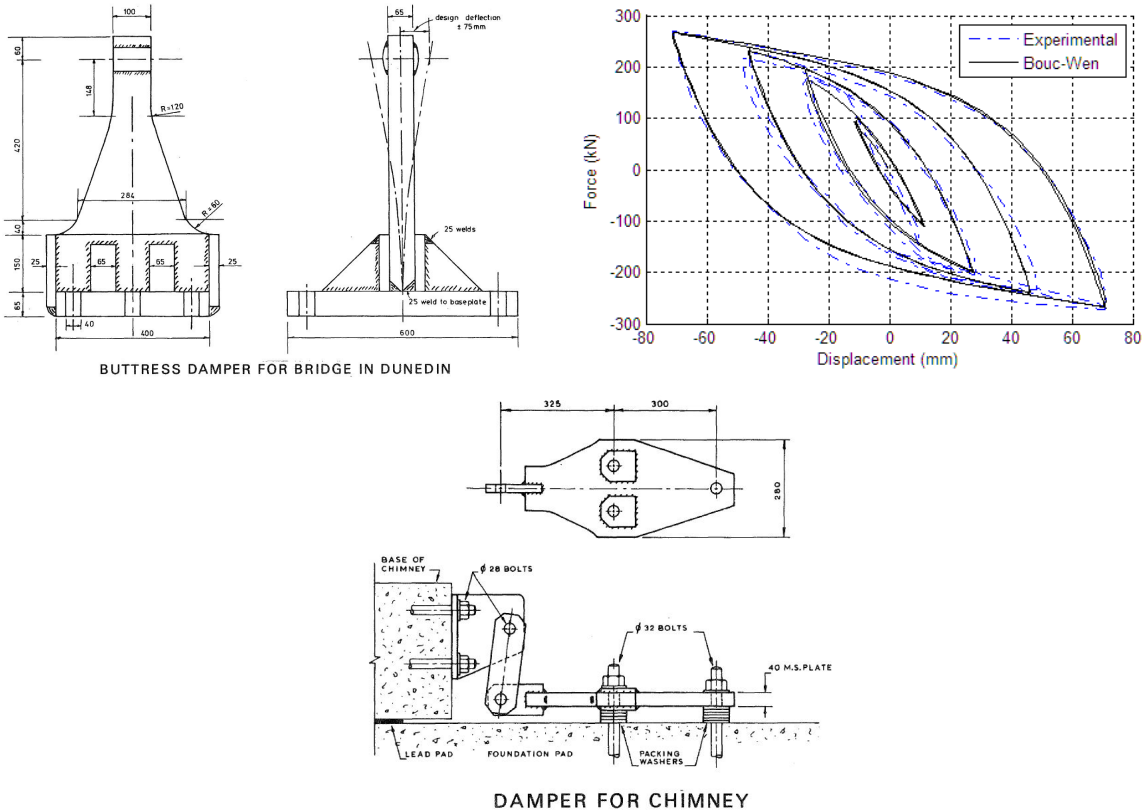

Figure 2. Top-left: Tapered plate damper used at the Dunedin Bridge in New Zealand (after Tyler, 1978). Top-right: best fit Bouc-Wen model compared to the Dunedin Bridge damper data. Bottom: side view of the Christchurch chimney tapered plate damper (after Tyler, 1978).

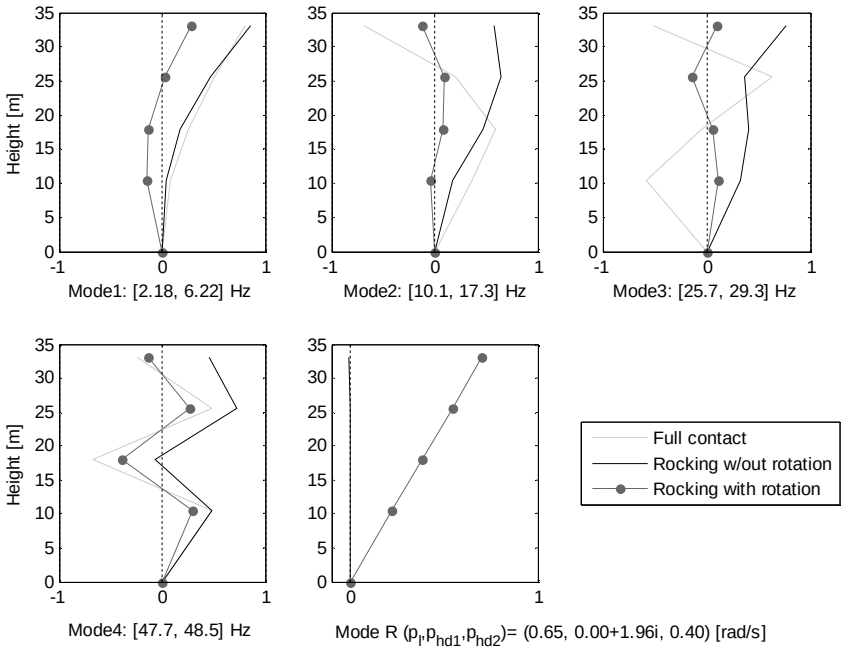

Figure 3. Modal analysis results for the Christchurch Chimney.

vibration characteristics between the two phases of motion decreases as the mode number increases, until the modal characteristics are nearly identical for the fourth mode.

The rigid body rocking mode (Mode R) is also depicted in Fig. 3, along with the related frequency parameter which results from the eigenvalue analysis (p_l = 0.65 rad/s). Interestingly, this frequency parameter is nearly identical to the frequency parameter which would be predicted using rigid body formulations, and approximates the pendulum frequency of the structure about the pivot axis. Also noted in Fig. 3 are the frequencies of Mode R if the stiffness of the hysteretic damper is included in the analysis as a bilinear elastic restrainer. Using the pre-yield stiffness, p_{hd1} becomes imaginary, indicating that the linearized system initially has a positive stiffness and a constant natural frequency of 0.31 Hz; using the post-yield stiffness, p_{hd2} = 0.40 rad/s, indicating that the system maintains a negative stiffness once full yielding occurs. The transition to positive rocking stiffness would only occur for a limited displacement range, although the system might attract more load due to increased stiffness. The decrease of the rocking post-yield stiffness frequency parameter ($p_{hd2} < p_l$), indicates that the dynamic resistance of the structure is increased by the dampers.

EARTHQUAKE RESPONSE

The response of the chimney was simulated using a variety of earthquake time histories to investigate the potential behavior of the designed chimney. Subsequently, the damper parameters and superstructure stiffness parameters were modified to investigate their influence on the total response.

Canterbury Aero Club Record

The chimney was first subjected to the Canterbury Aero Club time history that was recorded a few hundred meters from the chimney during the February 2011 Christchurch earthquake. For the unscaled record, the rocking response was found to be minimal, causing a damper displacement of less than 1 mm. This result agrees with the fact that no evidence of rocking was observed in the actual structure after the earthquake event (Sharpe and Grinlinton, 2013). Subsequently, the amplitude of the earthquake was increased to observe the response to larger ground motion shaking. When the acceleration amplitude was scaled by a factor of three, appreciable rocking was predicted (Fig. 4, left), although significant yielding of the damper was limited to one cycle (Fig. 4, bottom left). For the same earthquake acceleration scale factor of three, the simulation was repeated first for a hypothetical

chimney structure which is fixed to the ground and then for the chimney superstructure which is allowed to uplift, but with the hysteric dampers removed. The first simulation demonstrates the desired benefit of allowing rocking motion, a large reduction was observed in elastic displacements. Interestingly, for the second simulation, the response was found to be nearly identical (not shown), indicating that the dampers do not have any noticeable effect.

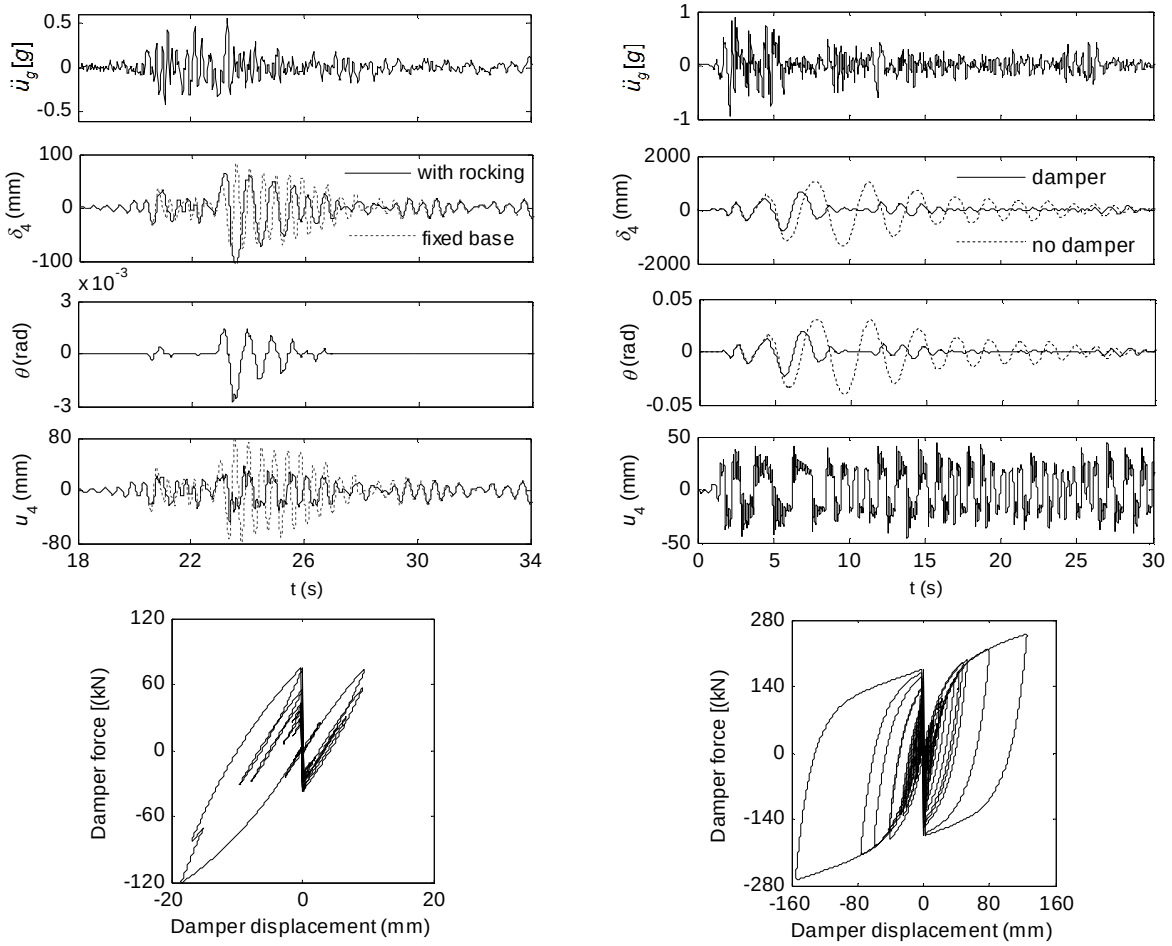

Figure 4. Example time history response of the chimney subjected to: (left) the Canterbury Aero Club record with amplitude scaled 3x, (right) the El Centro record with amplitude scaled 3x. In the bottom row, the response of the hysteretic dampers is depicted.

To investigate the effect of damper properties more generally, the acceleration amplitude of the earthquake was increased incrementally up to a scale factor (SF) of twenty. The results are plotted in Fig. 5. Although such drastic scaling is unrealistic, the results are interesting from the perspective of investigating the behaviour of the structure:

- For SF < 3, very little rocking occurred, but the elastic displacements were still noticeably reduced.
- Between 3 < SF < 9, significant rocking occurred, but the maximum displacements and the maximum rocking angle were nearly constant, as were the base shear and overturning moment. Thus, the structure was effectively isolated from the ground, and increasing the SF did not affect the force and displacement demand. Interestingly, the inclusion of the damper had almost no effect on the results, even though it was pushed to the estimated limit of where it could break ($\theta_{\max} / \alpha_{cg} = 0.05$, $d \approx 70$ mm).
- For SF > 9, the rocking angle increased dramatically, while the increase in elastic displacements was relatively minor. The base shear and overturning moments were

constant after a minor increase. However, the mid-height shear force and overturning moment continued to increase moderately with the scale factor. These mid-height values were half of the corresponding base values for SF < 9, but increase to be approximately equal to the corresponding base values at SF = 20. This surprising result may indicate a change in force distribution in the structure due to the increasing influence of a vibration mode response.

The inclusion of the damper, assuming it would never break, caused a significant reduction in rocking, while causing very little change to the base shear and the base overturning moment. Thus, the damper would ideally limit rocking motion without causing any additional force demand. In other words, the base isolation remains effective, but the total displacements are better controlled. However, to obtain these benefits the damper would have to be redesigned to increase its ductility.

El Centro Record

To investigate the response to a stronger earthquake record, and to compare with simulations conducted during the original design (Sharpe and Skinner, 1983), the chimney was also subjected to the N-S component of the El Centro earthquake recorded on 18 May, 1940. The analytical model predicted a maximum top displacement of 160 mm, very similar to the response predicted in the original design (Sharpe and Skinner, 1983). For the unscaled El Centro record, the response was also simulated with the damper removed, and the behavior was nearly identical (not shown).

Thus, again to investigate the importance of damping properties on the global response, the acceleration amplitude of the earthquake was incrementally increased up to a scale factor of six. An example result is presented in Fig. 4 (right) for an acceleration amplitude scale factor or 3, for the structure both with and without the damper. For this larger magnitude of response, the damper clearly limits rocking motion and particularly causes the rocking motion to die out rapidly instead of continuing for longer durations. On the contrary, the elastic response is relatively unaffected by the presence of the damper. The results for the entire range of scale factors considered are plotted in Fig. 6. The trends are similar to those observed in Fig. 5, but the various regimes of response occur for lower scale factors, and the continued increase in mid-height shear force and overturning moments was not observed.

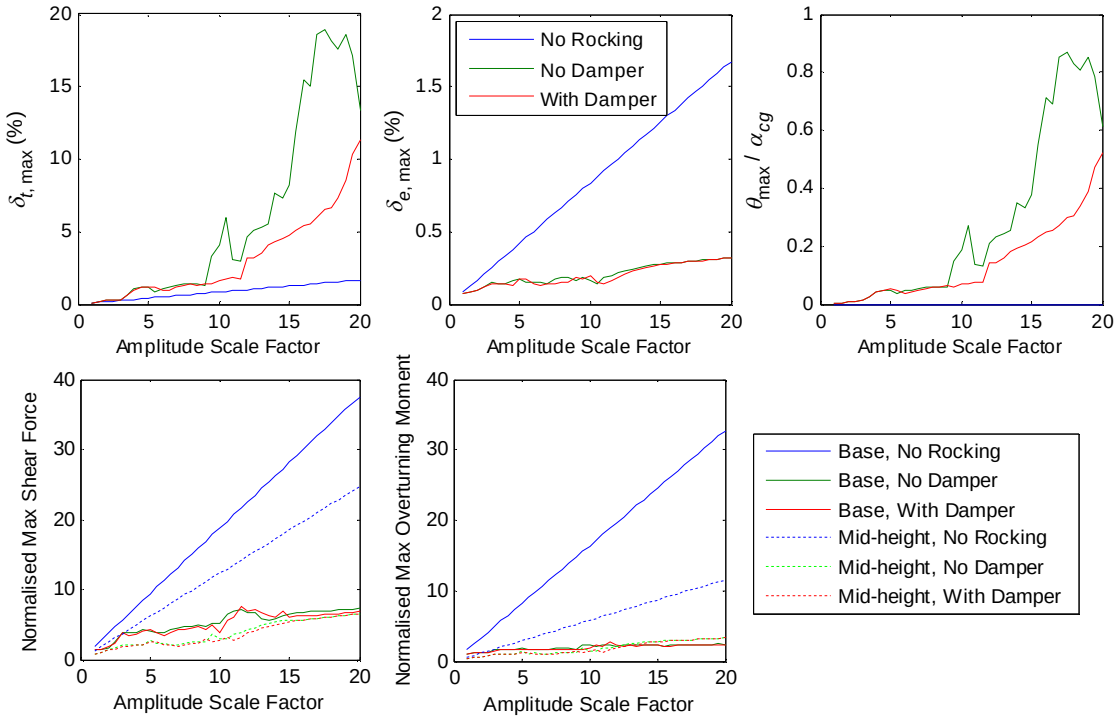

Figure 5. Incremental dynamic analysis using the Canterbury Aero Club earthquake record

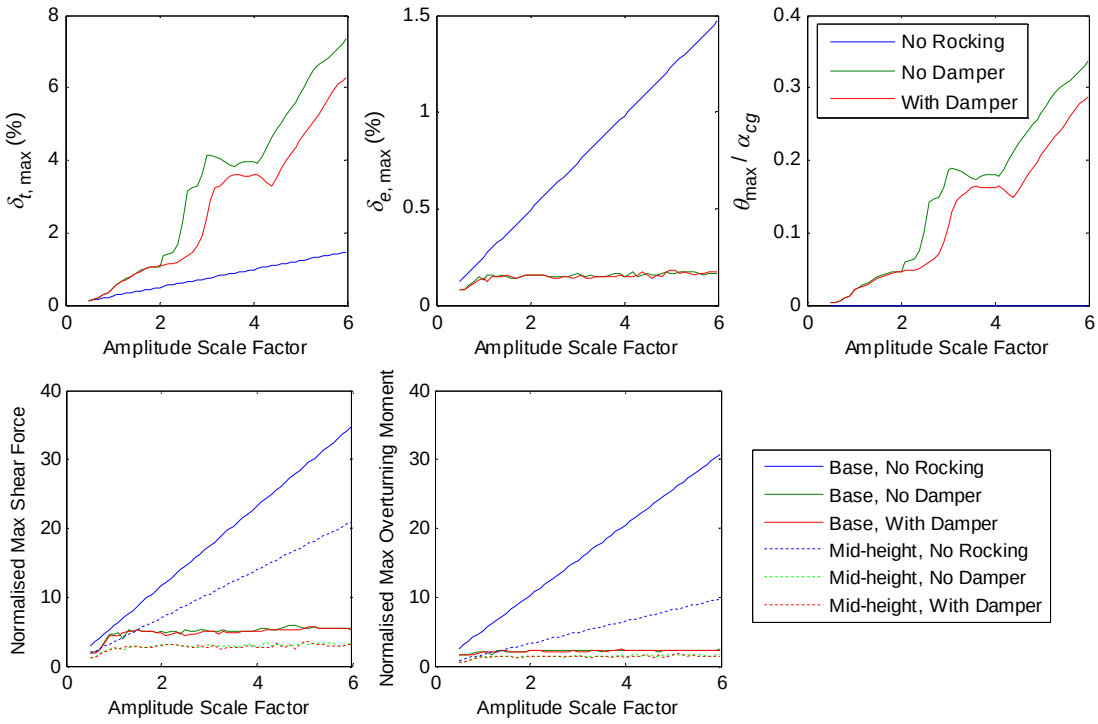

Figure 6. Incremental dynamic analysis using the El Centro earthquake record

PARAMETRIC STUDY

The results above indicate that rocking is certainly beneficial, but that the damper is of limited importance until very large ground motions occur. However, the dampers installed at the Christchurch Chimney are relatively weak. To preserve self-centering, the damper yield force must be less than half of the weight of the chimney. The installed dampers yield at ~6.7% of the weight of the structure.

To investigate the effect of the damper parameters, the thickness of the damper was incrementally increased, which results in a related increase in damper stiffness and strength. The results of the related incremental dynamic analysis using the Christchurch Aero Club record are presented in Fig. 7. For SF < 3, little rocking occurs and the damper makes no difference. For 3 < SF < 6, the increased stiffness of the thickest damper causes a moderate decrease in total displacement and rocking angle. For 6 < SF < 10, the damper thickness has no effect but to increase the base overturning moment, so there is no benefit to increasing the thickness. However, for SF > 10, the rocking amplitudes begin to increase dramatically, and now the increased strength of the thicker dampers began to cause an appreciable decrease in the maximum rocking response. However, the maximum elastic top displacements are less affected. Relatedly, the maximum shear force and base overturning moment are influenced relatively little, and inconsistently, by the change in damper properties.

In addition to having relatively weak dampers, the chimney itself is relatively stiff. Thus, the modal frequencies are relatively high, and the ground motion is unlikely to excite higher modes of the structure directly. However, for less stiff structures this may not be the case. Thus, to investigate the effect of the flexibility of the structure on the damped rocking response, the superstructure bending stiffness (*EI*) was also scaled incrementally. The results are shown in Fig. 8.

A reduction in stiffness had the expected effect of increasing the elastic displacements at the top of the structure, while the maximum rocking response was less, and inconsistently, affected. The effect of the superstructure stiffness on the maximum shear force and overturning moment was surprisingly inconsistent. If rocking was providing pure base isolation, then a change in superstructure stiffness would have a relatively small effect on the shear forces and bending moments (as in Figs. 5,6). Instead, it seems that the uplifted vibration modes were being excited and were causing an unexpectedly large response.

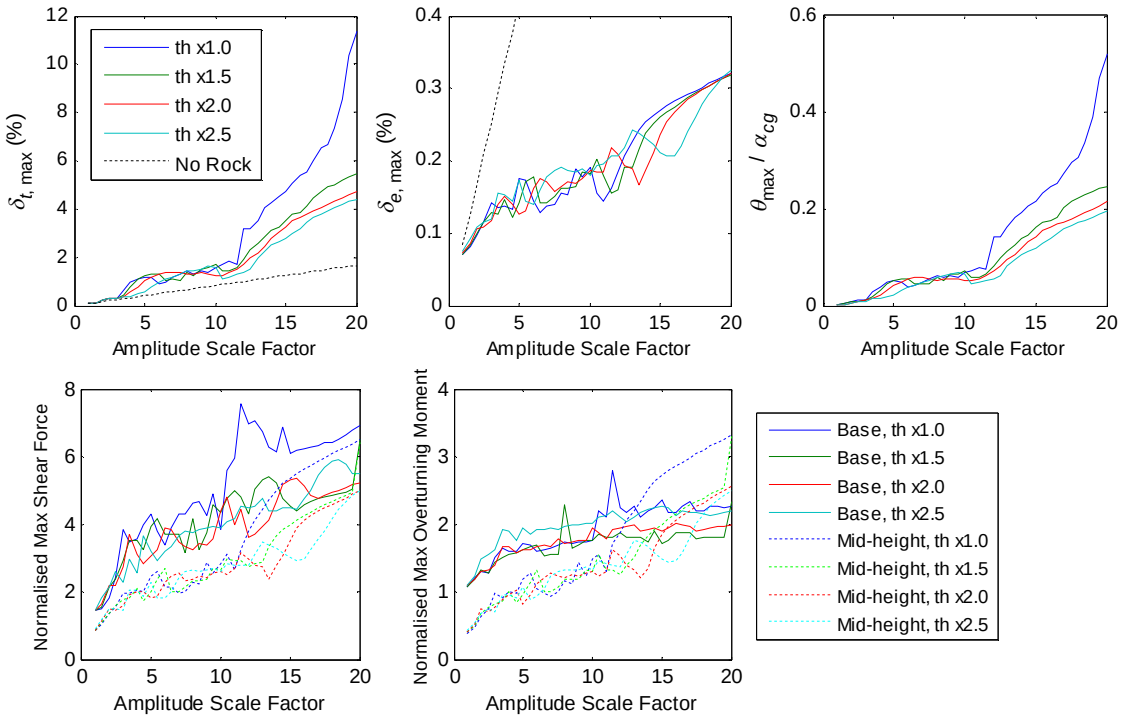

Figure 7. Incremental dynamic analysis for incrementally increasing damper thickness (th) using the Christchurch Aero Club record

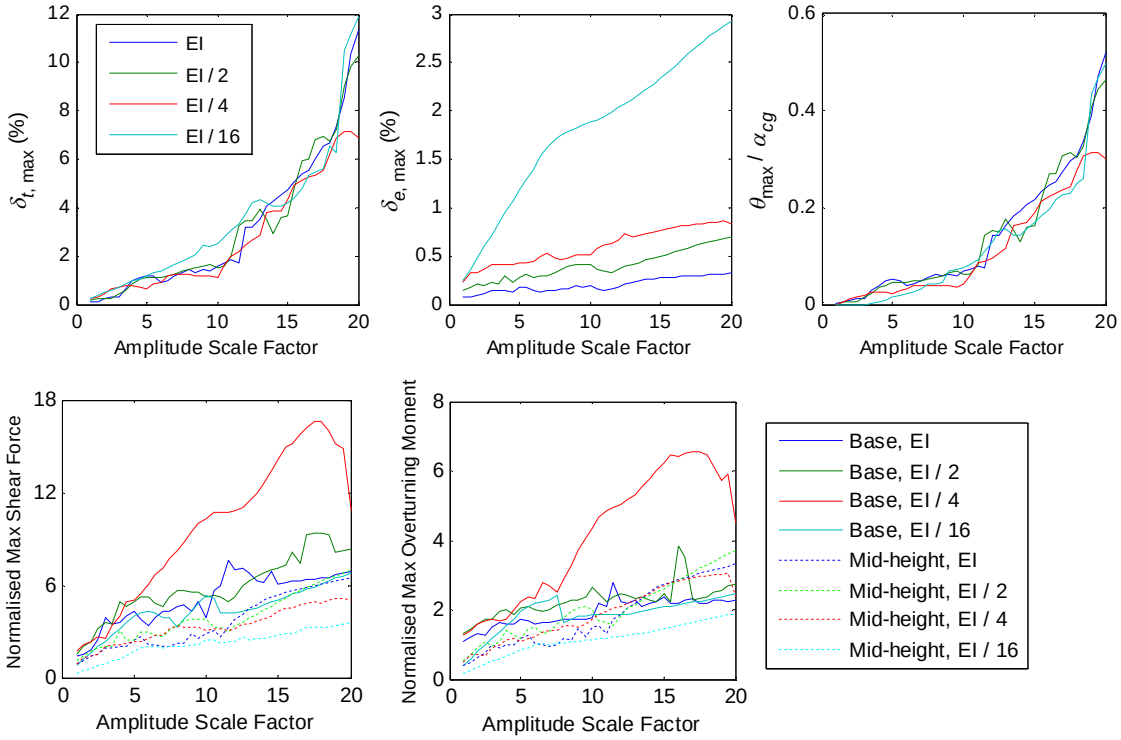

Figure 8. Incremental dynamic analysis for incrementally increasing stiffness of the superstructure using the Christchurch Aero Club record

CONCLUSIONS

This paper considers the importance of the yielding steel dissipaters to the seismic response of the Christchurch Chimney. The behaviour of the dissipaters was captured using a Bouc-Wen model, which was implemented within an existing analytical model for flexible rocking structures. Simulation of the seismic response agreed well with previous work, and confirmed that almost no rocking should have been expected to occur in the February 2011 Christchurch earthquake.

For increasing amplitudes of ground motion, the dampers were found to have almost no effect for expected levels of ground shaking. This was due to the scale of the structure, and may not be true for smaller scale structures with larger dampers. For very high levels of shaking, the inclusion of dampers would have effectively limited maximum rotations (if their ductility were increased), while having a relatively small effect on the shear forces and overturning moments. For these higher levels of shaking, increasing the thickness of the damper was found to be an effective way of further limiting maximum rotations. While for the original chimney configuration rocking isolated the superstructure vibrations, more flexible configurations indicated that unexpectedly large shear and bending forces may occur. This may be due to the direct excitation of vibration modes due to earthquake motion during rocking, suggesting that rocking isolation may have been partially effective for these modes.

ACKNOWLEDGEMENTS

The authors would like to thank Richard Sharpe of BECA and Air New Zealand for providing them with the construction drawings of the Christchurch Chimney.

REFERENCES

Acikgoz S and DeJong MJ (2012) “The interaction of elasticity and rocking in flexible structures allowed to uplift”, *Earthquake Engineering & Structural Dynamics*, 41(15): 2177-2194

Acikgoz S and DeJong MJ (2013) “Linearization and Modal Analysis of Flexible Rocking Structures”, *Proceedings of NZSEE Conference*, Wellington, New Zealand

Acikgoz S, Ma QT, Palermo A, DeJong MJ (2014) “Dynamic Characteristics of a Flexible Rocking Structure: Experimental Identification”, under review.

Acikgoz S and DeJong MJ (2014) “Dynamic Characteristics of a Flexible Rocking Structure: Analytical Modelling”, under review.

Hajjar JF, Sesen AH, Jampole E, Wetherbee A (2013) A synopsis of sustainable structural systems with rocking, self-centering, and articulated energy dissipating fuses, Report No. NEU-CEE-2013-01, Dept of Civil & Env. Engineering, Northeastern University, Boston, Massachusetts.

Shampine LF, Gladwell I, Thompson S (2003) “Solving ODEs with MATLAB”, Cambridge University Press

Sharpe RD and Grinlinton KE (2013) “Should the chimney have rocked?”, *Proceedings of NZSEE Conference*, Wellington, New Zealand

Sharpe RD and Skinner RI (1983) “The Seismic Design of an Industrial Chimney with Rocking Base”, *Bulletin of the New Zealand National Society for Earthquake Engineering*, 16(2): 98-106

Toranzo-Dianderas LA (2002) “The Use of Rocking Walls in Confined Masonry Structures: A Performance-based Approach”, Ph.D. Dissertation, University of Canterbury

Tyler RG (1978) “Tapered steel energy dissipators for earthquake resistant structures”, *Bulletin of the New Zealand National Society for Earthquake Engineering*, 11(4): 282-294

Wen YK (1976) “Method for Random Vibration of Hysteretic Systems”, *Journal of the Engineering Mechanics Division - ASCE*, 102(2): 249-263

Wiebe L, Christopoulos C, Tremblay R, Leclerc M (2013) “Mechanisms to limit higher mode effects in a controlled rocking steel frame. 2: Large‐amplitude shake table testing”, Earthquake Engineering & Structural Dynamics, 42(7): 1069-1086

Yim SCS and Chopra AK (1985) “Simplified earthquake analysis of multistory structures with foundation uplift”, Journal of Structural Engineering, 111(12): 2708–2731